PROCEEDINGS OF THE ROYAL SOCIETY A MATHEMATICAL, PHYSICAL & ENGINEERING SCIENCES

Electromechanical phase transition in dielectric elastomers

Rui Huang and Zhigang Suo

Proc. R. Soc. A 2012 **468**, 1014-1040 first published online 30 November 2011
doi: 10.1098/rspa.2011.0452

PROCEEDINGS OF THE ROYAL SOCIETY A

Proc. R. Soc. A (2012) **468**, 1014–1040
doi:10.1098/rspa.2011.0452
Published online 30 November 2011

Electromechanical phase transition in dielectric elastomers

By Rui Huang[1,*] and Zhigang Suo[2]

[1]*Department of Aerospace Engineering and Engineering Mechanics, University of Texas, Austin, TX 78712, USA*
[2]*School of Engineering and Applied Sciences, Harvard University, Cambridge, MA 02138, USA*

Subject to forces and voltage, a dielectric elastomer may undergo electromechanical phase transition. A phase diagram is constructed for an ideal dielectric elastomer membrane under uniaxial force and voltage, reminiscent of the phase diagram for liquid–vapour transition of a pure substance. We identify a critical point for the electromechanical phase transition. Two states of deformation (thick and thin) may coexist during the phase transition, with the mismatch in lateral stretch accommodated by wrinkling of the membrane in the thin state. The processes of electromechanical phase transition under various conditions are discussed. A reversible cycle is suggested for electromechanical energy conversion using the dielectric elastomer membrane, analogous to the classical Carnot cycle for a heat engine. The amount of energy conversion, however, is limited by failure of the dielectric elastomer owing to electrical breakdown. With a particular combination of material properties, the electromechanical energy conversion can be significantly extended by taking advantage of the phase transition without electrical breakdown.

Keywords: dielectric elastomer; phase transition; electromechanical instability; energy conversion; electrical breakdown

1. Introduction

While machines in engineering mostly use hard materials, machines in nature are often soft. Familiar examples include the accommodation of the eye, the beating of the heart, the sound shaped by the vocal folds and the sound in the ear. An exciting field of engineering is emerging that uses soft active materials to create soft machines (Calvert 2009; Suo 2010). Indeed, many soft materials are apt to mimic the salient feature of life: deformation in response to stimuli. An electric field can cause an elastomer to stretch several times its length (Pelrine *et al.* 2000; Ha *et al.* 2007; Carpi *et al.* 2010). A change in pH can cause a hydrogel to swell many times its volume (Liu & Urban 2010). These soft active materials are being developed for diverse applications, including soft robots, adaptive optics, self-regulating fluidics, programmable haptic surfaces and oil field management.

*Author for correspondence (ruihuang@mail.utexas.edu).

Received 26 July 2011
Accepted 1 November 2011

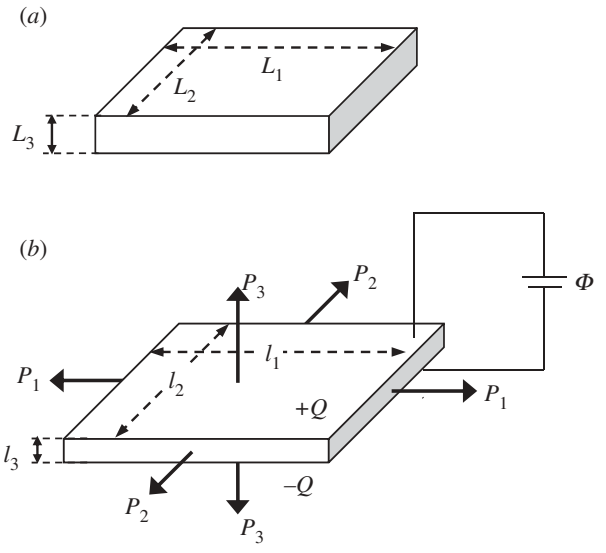

Figure 1. Schematic of a dielectric elastomer membrane, (*a*) reference state; (*b*) current state, subject to forces and an electric voltage.

As one particular class of soft active materials, dielectric elastomers are being developed intensely as transducers in many applications (Shankar *et al.* 2007; Carpi *et al.* 2008; Brochu & Pei 2010; Suo 2010). Figure 1 illustrates the principle of operation for a dielectric elastomer transducer. A membrane of a dielectric elastomer is sandwiched between two compliant electrodes. The electrodes have negligible electrical resistance and mechanical stiffness; a commonly used material for such electrodes is carbon grease. The dielectric elastomer is subject to forces and voltage. Charges flow through an external conducting wire from one electrode to the other. The charges of opposite signs on the two electrodes cause the membrane to deform. It was discovered that an applied voltage may cause dielectric elastomers to strain over 100 per cent (Pelrine *et al.* 2000). As a result, electric energy may be converted to do mechanical work and vice versa.

Electromechanical instability has been recognized as a mode of failure for dielectric elastomers subject to increasing voltage (Stark & Garton 1955; Plante & Dubowsky 2006), which limits the amount of energy conversion by dielectric elastomers in practical applications (Zhao & Suo 2007; Diaz-Calleja *et al.* 2008; Koh *et al.* 2009, 2011; Leng *et al.* 2009; Tommasi *et al.* 2010; Xu *et al.* 2010). In particular, an experimental manifestation of the electromechanical instability was reported by Plante & Dubowsky (2006): under a particular voltage, a pre-stretched dielectric elastomer membrane deformed into a complex pattern with a mixture of two states, one being flat and the other wrinkled. This phenomenon has been interpreted as coexistence of the two states owing to a non-convex free-energy function of the dielectric elastomer, which leads to a discontinuous phase transition (Zhao *et al.* 2007; Zhou *et al.* 2008). In one state, the membrane is thick and has a small in-plane stretch. In the other state, the membrane is thin and has a large in-plane stretch. The two states may coexist at a specific voltage, so that some regions of the membrane are in the thick state,

while other regions are in the thin state. To accommodate the mismatch of in-plane stretches in the two states, the membrane wrinkles in the regions of the thin state.

While the electromechanical phase transition often leads to failure of the dielectric elastomer transducers, it may offer an enabling mechanism for electromechanical energy conversion, analogous to the liquid–vapour phase transition in a steam engine. For this purpose, it is essential to understand the processes of electromechanical phase transition in dielectric elastomers along with the physical limits set by pertinent failure modes. In this paper, we present a theoretical analysis on the electromechanical phase transition in dielectric elastomers under various loading conditions. In particular, a phase diagram is constructed for an ideal dielectric elastomer subject to uniaxial force and voltage, which closely resembles the liquid–vapour phase transition of a pure substance. On the phase diagram, we identify a critical point of the electromechanical phase transition. The membrane can change from a thick state to a thin state by a discontinuous phase transition along a subcritical loading path. Alternatively, the membrane can change from a thick state to a thin state by a succession of gradual changes along a supercritical loading path. By allowing electromechanical phase transition, one may significantly enhance the amount of energy conversion by the dielectric elastomer transducers.

The remainder of this paper is organized as follows. Section 2 presents the equations of state for an ideal dielectric elastomer. In §3, solutions are presented for homogeneous deformation of a dielectric elastomer under uniaxial force and voltage. The stability of a homogeneous deformation state against small perturbations is discussed in §4. Section 5 presents an analysis of electromechanical phase transition along with graphical representations of the phase diagram. In §6, two specific processes of phase transition are discussed, a reversible process cycle is suggested for electromechanical energy conversion, and the physical limit for energy conversion set by electrical breakdown of the dielectric elastomer is discussed. Section 7 concludes the present study with a brief summary.

2. Equations of state

The theory of dielectric elastomers has been developed in various forms (e.g. Dorfmann & Ogden 2005; Goulbourne *et al.* 2005; McMeeking & Landis 2005; Suo *et al.* 2008; Trimarco 2009). This section reviews the equations of state, following the notation in Suo *et al.* (2008).

(*a*) *Free energy and condition of equilibrium*

With reference to figure 1, consider a membrane of dielectric elastomer, sandwiched between two compliant electrodes. In the reference state, the membrane is subject to neither force nor voltage, and is of dimensions L_1, L_2 and L_3. In the current state, the membrane is subject to forces P_1, P_2 and P_3, while the two electrodes are connected through a conducting wire to a battery of voltage Φ. In the current state, the dimensions of the membrane become l_1, l_2 and l_3, and the two electrodes accumulate charges $\pm Q$.

Deformation of the elastomer is entropic, and we consider isothermal processes in the present study. Denote the Helmholtz free energy of the elastomer in the current state by F, taken to be a function of four independent variables, $F(l_1, l_2, l_3, Q)$. The potential energy of the forces is $-P_1 l_1 - P_2 l_2 - P_3 l_3$, and the potential energy of the voltage is $-\Phi Q$. The elastomer membrane, the forces and the voltage together constitute a thermodynamic system. The free energy of this system, Π, consists of the Helmholtz free energy of the elastomer, the potential energy of the forces and the potential energy of the voltage:

$$\Pi = F(l_1, l_2, l_3, Q) - P_1 l_1 - P_2 l_2 - P_3 l_3 - \Phi Q. \tag{2.1}$$

When the forces and the voltage are fixed, the free energy of the system is a function of the four independent variables, $\Pi(l_1, l_2, l_3, Q)$. The state of equilibrium is then determined by minimizing the free energy with respect to the variables.

(*b*) *Incompressible dielectric elastomers*

For the time being, we assume that the membrane undergoes homogeneous deformation. Define the nominal density of the Helmholtz free energy by $W = F/(L_1, L_2, L_3)$, stretches by $\lambda_1 = l_1/L_1, \lambda_2 = l_2/L_2$ and $\lambda_3 = l_3/L_3$, stresses by $\sigma_1 = P_1/(l_2 l_3)$, $\sigma_2 = P_2/(l_1 l_3)$ and $\sigma_3 = P_3/(l_1 l_2)$, electrical field by $E = \Phi/l_3$, and electrical displacement by $D = Q/(l_1 l_2)$.

When an elastomer undergoes large deformation, the change in the shape of the elastomer is typically much more significant than the change in the volume. Consequently, the volume of the elastomer is often taken to remain unchanged during deformation such that

$$\lambda_1 \lambda_2 \lambda_3 = 1. \tag{2.2}$$

Under this assumption of incompressibility, the three stretches are no longer independent. We regard λ_1 and λ_2, along with D, as three independent variables that describe the state of the elastomer.

As a model of an incompressible dielectric elastomer, the nominal density of the Helmholtz free energy is assumed to be a function of the three independent variables:

$$W = W(\lambda_1, \lambda_2, D). \tag{2.3}$$

The free energy of the system in (2.1) can then be written in terms of the same variables:

$$\begin{aligned}\Pi(\lambda_1, \lambda_2, D) = {} & L_1 L_2 L_3 W(\lambda_1, \lambda_2, D) - P_1 L_1 \lambda_1 - P_2 L_2 \lambda_2 \\ & - P_3 L_3 \lambda_1^{-1} \lambda_2^{-1} - \Phi L_1 L_2 \lambda_1 \lambda_2 D.\end{aligned} \tag{2.4}$$

When the forces and the voltage are fixed, a state of stable equilibrium is attained when the function $\Pi(\lambda_1, \lambda_2, D)$ is minimized with respect to the three independent variables.

Setting the first derivatives of the free-energy function to vanish, $\partial \Pi / \partial \lambda_1 = 0$, $\partial \Pi / \partial \lambda_2 = 0$ and $\partial \Pi / \partial D = 0$, we obtain that

$$\sigma_1 - \sigma_3 + ED = \lambda_1 \frac{\partial W(\lambda_1, \lambda_2, D)}{\partial \lambda_1}, \tag{2.5}$$

$$\sigma_2 - \sigma_3 + ED = \lambda_2 \frac{\partial W(\lambda_1, \lambda_2, D)}{\partial \lambda_2} \tag{2.6}$$

and

$$E = \frac{\partial W(\lambda_1, \lambda_2, D)}{\partial D}. \tag{2.7}$$

Once the function $W(\lambda_1, \lambda_2, D)$ is specified for the incompressible dielectric elastomer, the four equations, (2.2) and (2.5)–(2.7), constitute the equations of state. We note however that (2.5)–(2.7) are necessary but not sufficient to minimize the free energy Π. As a result, the equilibrium state described by these equations may be stable or unstable. The stability of the equilibrium state will be discussed in §4.

(*c*) *Ideal dielectric elastomers*

The free energy in (2.4) suggests two types of electromechanical coupling: the coupling resulting from the geometric relationship between the charge and the stretches, $Q = L_1 L_2 \lambda_1 \lambda_2 D$, and the coupling resulting from the function $W(\lambda_1, \lambda_2, D)$. An elastomer is a three-dimensional network of long and flexible polymer chains, held together by covalent cross-links. Each polymer chain consists of a large number of monomers. Consequently, the cross-links have negligible effect on the polarization of the monomers—that is, the elastomer can polarize nearly as freely as a polymer melt. This simple molecular picture is consistent with the following experimental observation: the permittivity changes by only a few percent when a membrane of an elastomer is stretched to increase the area by 25 times (Kofod *et al.* 2003).

As an idealization, the dielectric behaviour of an elastomer is assumed to be exactly the same as that of a polymer melt—that is, the true electric field relates to the true electric displacement as:

$$D = \varepsilon E, \tag{2.8}$$

where ε is the permittivity of the elastomer, taken to be a constant independent of deformation. We note that in general the permittivity of an elastomer may depend on deformation, especially at an extremely large stretch.

Using (2.8) and integrating (2.7) with respect to D, we obtain that

$$W = W_{\mathrm{s}}(\lambda_1, \lambda_2) + \frac{D^2}{2\varepsilon}. \tag{2.9}$$

The constant of integration, $W_{\mathrm{s}}(\lambda_1, \lambda_2)$, is the Helmholtz free energy associated with stretching of the elastomer, and the term $D^2/(2\varepsilon)$ is the Helmholtz free energy associated with polarization. In this model, the stretches and the polarization contribute to the free energy independently. Consequently, the electromechanical coupling is purely a geometric effect associated with the expression $Q = L_1 L_2 \lambda_1 \lambda_2 D$. This material model is known as the model of ideal dielectric elastomers (Zhao *et al.* 2007).

For a membrane of an incompressible, ideal dielectric elastomer, with (2.8) and (2.9), the free energy of the system in (2.4) can now be written in the form

$$\frac{\Pi}{L_1L_2L_3} = W_s(\lambda_1,\lambda_2) - \frac{P_1}{L_2L_3}\lambda_1 - \frac{P_2}{L_3L_1}\lambda_2 - \frac{P_3}{L_1L_2}\lambda_1^{-1}\lambda_2^{-1} - \frac{\varepsilon}{2}\left(\frac{\Phi}{L_3}\right)^2(\lambda_1\lambda_2)^2. \tag{2.10}$$

When the forces and the voltage are fixed, the free energy in (2.10) is a function of the two stretches, $\Pi(\lambda_1,\lambda_2)$. A state of stable equilibrium is attained when the function $\Pi(\lambda_1,\lambda_2)$ is minimized.

Again, setting the first derivatives of the free energy in (2.10) to vanish, $\partial\Pi/\partial\lambda_1 = 0$ and $\partial\Pi/\partial\lambda_2 = 0$, we obtain that

$$\sigma_1 - \sigma_3 + \varepsilon E^2 = \lambda_1\frac{\partial W_s(\lambda_1,\lambda_2)}{\partial\lambda_1} \tag{2.11}$$

and

$$\sigma_2 - \sigma_3 + \varepsilon E^2 = \lambda_2\frac{\partial W_s(\lambda_1,\lambda_2)}{\partial\lambda_2}. \tag{2.12}$$

These two equations are commonly justified by identifying εE^2 as the Maxwell stress (e.g. Goulbourne *et al.* 2005; Wissler & Mazza 2005; Plante & Dubowsky 2006). Apparently, the Maxwell stress accounts for electromechanical coupling in incompressible elastomers with liquid-like dielectric behaviour (Suo *et al.* 2008). The general procedure as described above, however, has been extended to other kinds of elastic dielectrics, as reviewed in Suo (2010).

(*d*) *Limiting stretches*

The free energy due to elastic stretching, $W_s(\lambda_1,\lambda_2)$, may be selected from a large menu of well-tested functions in the literature of rubber elasticity (Boyce & Arruda, 2000). A behaviour of particular significance to electromechanical instability is stiffening of an elastomer at large stretches. In an elastomer, each individual polymer chain has a finite contour length. When the elastomer is subject to no load, the polymer chains are coiled, allowing a large number of conformations. When stretched, the end-to-end distance of each polymer chain increases and eventually approaches the finite contour length, setting up a limiting stretch. On approaching the limiting stretch, the elastomer stiffens steeply.

To take into account the effect of limiting stretches, we use Gent's free energy function (Gent 1996):

$$W_s(\lambda_1,\lambda_2) = -\frac{\mu J_{\lim}}{2}\log\left(1 - \frac{\lambda_1^2+\lambda_2^2+\lambda_1^{-2}\lambda_2^{-2}-3}{J_{\lim}}\right), \tag{2.13}$$

where μ is the small-stress shear modulus, and $J_{\lim}$ is a dimensionless parameter related to the limiting stretch. By the functional form in (2.13), the stretches are restricted by the condition, $0 \le (\lambda_1^2+\lambda_2^2+\lambda_1^{-2}\lambda_2^{-2}-3)/J_{\lim} < 1$. When deformation is small compared with the limiting stretch, $(\lambda_1^2+\lambda_2^2+\lambda_1^{-2}\lambda_2^{-2}-3)/J_{\lim} \to 0$, and the Taylor expansion of (2.13) recovers the free-energy function for the incompressible neo-Hookean model: $W_s = (\mu/2)(\lambda_1^2+\lambda_2^2+\lambda_1^{-2}\lambda_2^{-2}-3)$. When the elastomer approaches the limiting stretch, $(\lambda_1^2+$

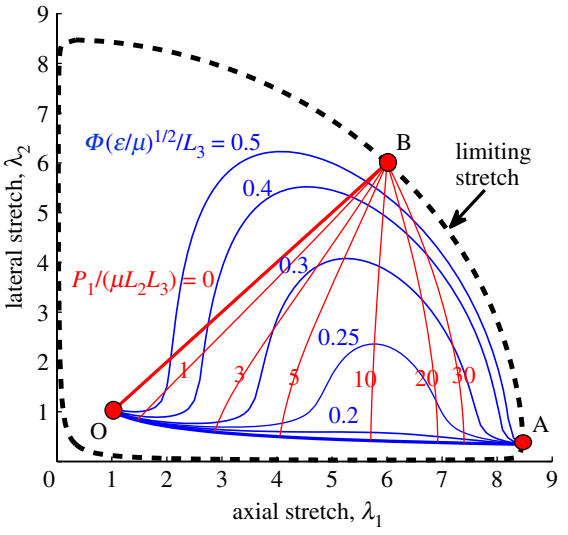

Figure 2. Curves of constant voltage and curves of constant axial force on the (λ_1, λ_2) plane for a dielectric elastomer membrane. The dashed curve is the boundary set by equation (2.14) for the limiting stretch of the elastomer ($J_{\lim} = 69$). (Online version in colour.)

$\lambda_2^2 + \lambda_1^{-2}\lambda_2^{-2} - 3)/J_{\lim} \to 1$, the free energy (2.13) diverges, and the stiffness of the elastomer becomes unbounded. Therefore, the condition for the limiting stretch is

$$\lambda_1^2 + \lambda_2^2 + \lambda_1^{-2}\lambda_2^{-2} - 3 = J_{\lim}. \tag{2.14}$$

Condition (2.14) is plotted in figure 2 on the (λ_1, λ_2) plane as the dashed curve. Unless otherwise noted, in presenting numerical results, we set $J_{\lim} = 69$ throughout this paper. In figure 2, point O represents the unstretched state ($\lambda_1 = \lambda_2 = 1$), whereas points A and B represent the limiting stretches under two different loading conditions. Point A corresponds to the limiting stretch for the elastomer subject to uniaxial force but subject to no voltage ($\Phi = 0$), for which the lateral stretch is related to the axial stretch as $\lambda_2 = \sqrt{1/\lambda_1}$. Thus, equation (2.14) reduces to

$$\lambda_1^2 + \frac{2}{\lambda_1} = J_{\lim} + 3, \tag{2.15}$$

which gives the limiting stretch in the axial direction, $\lambda_1^{\mathrm{A}} = 8.5$ for $J_{\lim} = 69$. Point B corresponds to the limiting stretch under equal-biaxial condition ($\lambda_1 = \lambda_2$), for which equation (2.14) becomes

$$2\lambda_1^2 + \frac{1}{\lambda_1^4} = J_{\lim} + 3, \tag{2.16}$$

and for $J_{\lim} = 69$ we obtain the stretch, $\lambda_1^{\mathrm{B}} = 6$. Thus, the value of $J_{\lim}$ can be determined by measuring one of the limiting stretches. Once $J_{\lim}$ is known, condition (2.14) sets the boundary on the (λ_1, λ_2) plane for all possible deformation states of the elastomer, regardless of the loading conditions.

With function (2.13), the equilibrium conditions in (2.11) and (2.12) become

$$\sigma_1 - \sigma_3 + \varepsilon E^2 = \frac{\mu(\lambda_1^2 - \lambda_1^{-2}\lambda_2^{-2})}{1 - (\lambda_1^2 + \lambda_2^2 + \lambda_1^{-2}\lambda_2^{-2} - 3)/J_{\lim}} \tag{2.17}$$

and

$$\sigma_2 - \sigma_3 + \varepsilon E^2 = \frac{\mu(\lambda_2^2 - \lambda_1^{-2}\lambda_2^{-2})}{1 - (\lambda_1^2 + \lambda_2^2 + \lambda_1^{-2}\lambda_2^{-2} - 3)/J_{\lim}}. \tag{2.18}$$

Equations (2.2), (2.8), (2.17) and (2.18) constitute a complete set of equations of state for the specific material model of dielectric elastomers, which we use in the following analysis.

3. Homogeneous deformation

To be specific, we consider a dielectric elastomer membrane subject to a voltage Φ and a uniaxial force P_1, while $P_2 = P_3 = 0$. Recall that the stress $\sigma_1 = P_1/(l_2 l_3) = \lambda_1 P_1/(L_2 L_3)$ and the electric field $E = \Phi/l_3 = \lambda_1\lambda_2\Phi/L_3$. With $\sigma_2 = \sigma_3 = 0$, we rewrite (2.17) and (2.18) in a dimensionless form:

$$\frac{P_1}{\mu L_2 L_3} = \frac{\lambda_1 - \lambda_1^{-1}\lambda_2^2}{1 - (\lambda_1^2 + \lambda_2^2 + \lambda_1^{-2}\lambda_2^{-2} - 3)/J_{\lim}} \tag{3.1}$$

and

$$\left(\frac{\Phi}{L_3}\sqrt{\frac{\varepsilon}{\mu}}\right)^2 = \frac{\lambda_1^{-2} - \lambda_1^{-4}\lambda_2^{-4}}{1 - (\lambda_1^2 + \lambda_2^2 + \lambda_1^{-2}\lambda_2^{-2} - 3)/J_{\lim}}. \tag{3.2}$$

In obtaining (3.1), we have taken the difference between (2.17) and (2.18). The normalized force $P_1/(\mu L_2 L_3)$ and the normalized voltage $\Phi/(L_3\sqrt{\mu/\varepsilon})$ are the dimensionless loading parameters. Once the two loading parameters are prescribed, (3.1) and (3.2) are coupled nonlinear equations that determine the stretches λ_1 and λ_2 in the current state of the elastomer membrane, assuming homogeneous deformation.

We now return to the (λ_1, λ_2) plane in figure 2. Subject to a non-negative uniaxial force in the 1-direction ($P_1 \geq 0$) and a voltage, the deformation state of the elastomer membrane is restricted to a region bounded by three curves: the limiting-stretch curve AB, the zero-voltage curve OA and the equi-biaxial curve OB. We plot (3.1) as curves of constant forces and plot (3.2) as curves of constant voltages. All curves of constant forces start from a point on the zero-voltage curve OA and meet at point B, the equal-biaxial limiting stretch. The equi-biaxial curve OB is also the curve of zero axial force. Regardless of the magnitude of the axial force, point B is approached when the applied voltage is sufficiently high. Similarly, all curves of constant voltages start from a point on the zero force curve OB (close to but not exactly point O) and meet at point A, the limiting stretch caused by the uniaxial force alone. Point A is approached when the axial force is sufficiently high, regardless of the voltage. Some curves of constant voltages go beyond the zero-force curve OB, which would require a compressive force ($P_1 < 0$) and is thus practically unattainable as the membrane typically has negligible resistance to buckling under compression.

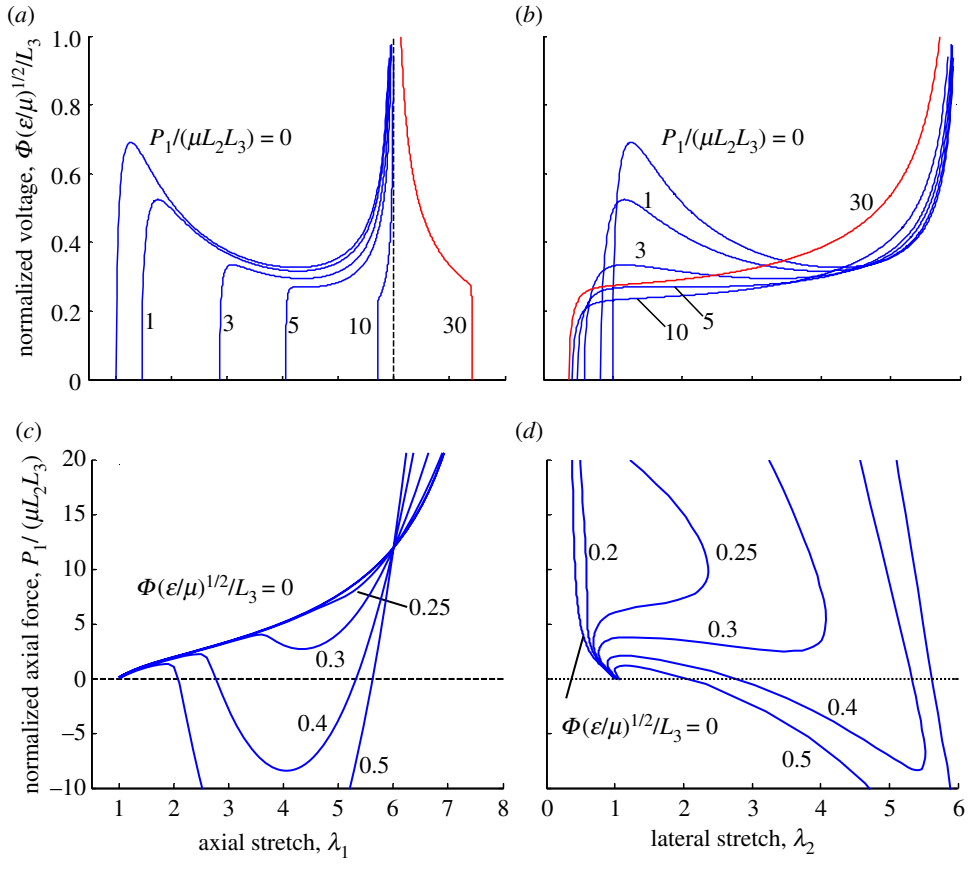

Figure 3. Stretches of a dielectric elastomer membrane caused by uniaxial force and voltage as predicted by the homogeneous solution. For constant values of the force: (*a*) $\Phi - \lambda_1$ and (*b*) $\Phi - \lambda_2$ curves. For constant values of the voltage: (*c*) $P_1 - \lambda_1$ and (*d*) $P_1 - \lambda_2$ curves. (Online version in colour.)

When a curve of constant force and a curve of constant voltage intersect on the (λ_1, λ_2) plane, the point of intersection represents a state of equilibrium for the elastomer subject to the specific combination of force and voltage. The state however could be stable, metastable or unstable. When a curve of constant force and a curve of constant voltage intersect at multiple points, more than one states exist for the force–voltage combination, which is indicative of instability and phase transition, to be discussed later.

Figure 3 plots the stretches of the elastomer membrane as functions of the uniaxial force and the voltage. Each curve in figure 3*a* may be interpreted as the axial stretch caused by variable voltage and a constant force (a dead weight). When the dead weight is small, e.g. $P_1/(\mu L_2 L_3) = 1$, the voltage as a function of the axial stretch first goes up, then down and then up again. The curve has a local maximum and a local minimum. The local maximum has long been associated with the electromechanical instability (Stark & Garton 1955). As the voltage increases, the membrane thins down, so that the same voltage induces an even

higher electric field. This positive feedback results in the local maximum of the $\Phi - \lambda_1$ curve. The local minimum results from the requirement that the voltage diverges as the membrane approaches the equal-biaxial limiting stretch. This trend was identified by Zhao *et al.* (2007) and was linked to electromechanical phase transition, as discussed further in §5.

As the dead weight increases, the maximum voltage decreases and then disappears. This trend is understood as follows. Prior to applying the voltage, the large dead weight pulls the membrane, so that the membrane stiffens significantly as it approaches the limiting stretch. With a sufficiently large dead weight, the stiffening eliminates the local maximum in the $\Phi - \lambda_1$ curve and hence the electromechanical instability. This behaviour has been used to explain why pre-stretch increases the voltage-induced strains (Koh *et al.* 2011; Li *et al.* 2011), a well-known phenomenon observed experimentally by Pelrine *et al.* (2000).

We note a new behaviour when the dead weight is very large. As shown in figure 2, the limiting axial stretch under zero voltage ($\lambda_1^{\mathrm{A}} = 8.5$) is greater than the equi-biaxial limiting stretch ($\lambda_1^{\mathrm{B}} = 6$). Prior to applying the voltage, a large dead weight, e.g. $P_1/(\mu L_2 L_3) = 30$, stretches the membrane in the axial direction beyond the equi-biaxial limit ($\lambda_1 > \lambda_1^{\mathrm{B}}$). Subsequently, as the voltage ramps up, the axial stretch decreases to approach λ_1^{B}, as shown in figure 3*a*. That is, applying the voltage causes the membrane to contract in the axial direction, doing positive work by lifting the dead weight, a behaviour reminiscent of contractile muscles. We are unaware of any experimental observation of this contractile behaviour for dielectric elastomers.

Figure 3*b* plots the $\Phi - \lambda_2$ curves when the membranes are subject to constant uniaxial forces. For all positive values of the axial force, the lateral stretch is less than 1 at zero voltage and approaches the equal-biaxial limiting stretch ($\lambda_1^{\mathrm{B}} = 6$) at high voltage. When the axial force is relatively large, say, $P_1/(\mu L_2 L_3) = 10$, prior to applying the voltage, the axial stretch is close to the equi-biaxial limiting stretch, but the lateral stretch is far below the limiting stretch. Subsequently, when the voltage is applied, modest further stretch occurs in the axial direction, but a large further stretch occurs in the lateral direction. In other words, the relative axial stretch induced by the voltage is reduced by pre-stretching the elastomer with a constant force, while the relative stretch in the lateral direction is enlarged. This behaviour has been observed experimentally (Pelrine *et al.* 2000).

Figure 3*c* plots the axial force–stretch curves under constant voltages. When the voltage is low, e.g. $\Phi/(L_3\sqrt{\mu/\varepsilon}) = 0.25$, the axial stretch increases monotonically with the axial force. When the voltage is high, e.g. $\Phi/(L_3\sqrt{\mu/\varepsilon}) = 0.3$, however, the force as a function of the axial stretch has a local maximum and a local minimum, which is again indicative of instability and phase transition. When the voltage is even higher, e.g. $\Phi/(L_3\sqrt{\mu/\varepsilon}) = 0.4$, the force becomes negative (compression) for a range of axial stretch. However, owing to negligible bending stiffness of the membrane, the homogeneous state under compression is unstable and practically unattainable.

Figure 3*d* plots the lateral stretch versus the uniaxial force with constant voltages. When no voltage is applied ($\Phi = 0$), the elastomer under a positive axial force contracts in the lateral direction simply by Poisson's effect. For an incompressible elastomer, the lateral stretch is related to the axial stretch by $\lambda_2 = \sqrt{1/\lambda_1}$, which decreases monotonically as the axial force increases. When a constant voltage is applied, the lateral stretch depends on the combination of the

axial force and the voltage. With a relatively high voltage, e.g. $\Phi/(L_3\sqrt{\mu/\varepsilon}) = 0.3$, the lateral stretch as a function of the axial force first decreases, then increases and then decreases again. This behaviour may be understood as a result of competition between the axial force and the voltage: the axial force tends to decrease the lateral stretch while the voltage tends to increase the lateral stretch; the two effects combine in a nonlinear manner.

With the same equations of state, homogeneous deformation of dielectric elastomers under other loading conditions may be considered. In particular, when the elastomer membrane is subject to a uniaxial force under an open-circuit condition, the total charge on the electrodes is conserved while the voltage changes as the elastomer deforms. This condition is important in forming a complete process cycle for electromechanical energy conversion as discussed in §6. In some experiments, the elastomer membrane is fixed with a pre-stretch and then subject to an increasing voltage (Plante & Dubowsky 2006). In this case, as discussed in §6*a*, the axial force in the membrane relaxes with increasing voltage until it becomes zero. Further increasing the voltage would cause buckling of the membrane.

4. Stability of a homogeneous state against small perturbation

When a homogeneous deformation state (λ_1, λ_2) is perturbed to a nearby state $(\lambda_1 + \delta\lambda_1, \lambda_2 + \delta\lambda_2)$, the free energy of the system changes by $\delta\Pi = \Pi(\lambda_1 + \delta\lambda_1, \lambda_2 + \delta\lambda_2) - \Pi(\lambda_1, \lambda_2)$. Express this change in the Taylor series up to the second-order terms:

$$\delta\Pi = \frac{\partial\Pi}{\partial\lambda_1}\delta\lambda_1 + \frac{\partial\Pi}{\partial\lambda_2}\delta\lambda_2 + \frac{1}{2}\frac{\partial^2\Pi}{\partial\lambda_1^2}(\delta\lambda_1)^2 + \frac{1}{2}\frac{\partial^2\Pi}{\partial\lambda_2^2}(\delta\lambda_2)^2 + \frac{\partial^2\Pi}{\partial\lambda_1\delta\lambda_2}(\delta\lambda_1)(\delta\lambda_2). \quad (4.1)$$

For the state (λ_1, λ_2) to be an equilibrium state stable against an arbitrary small perturbation $(\delta\lambda_1, \delta\lambda_2)$, the free-energy function $\Pi(\lambda_1, \lambda_2)$ must be a local minimum. That is, the change in the free energy $\delta\Pi$ must be positive-definite for any small perturbation $(\delta\lambda_1, \delta\lambda_2)$. This requirement sets the first derivatives of the free energy to vanish, and the sum of the second-order terms in (4.1) to be positive-definite.

Setting the first derivatives in (4.1) to vanish, we recover (2.11) and (2.12). Requiring the sum of second-order terms to be positive-definite is equivalent to requiring that the Hessian matrix,

$$\mathbf{H} = \begin{bmatrix} \dfrac{\partial^2\Pi(\lambda_1,\lambda_2)}{\partial\lambda_1^2} & \dfrac{\partial^2\Pi(\lambda_1,\lambda_2)}{\partial\lambda_1\partial\lambda_2} \\ \dfrac{\partial^2\Pi(\lambda_1,\lambda_2)}{\partial\lambda_1\partial\lambda_2} & \dfrac{\partial^2\Pi(\lambda_1,\lambda_2)}{\partial\lambda_2^2} \end{bmatrix}, \quad (4.2)$$

be positive-definite. The transition from a local minimum to a saddle point for the free-energy function occurs when the determinant of the Hessian matrix becomes zero:

$$\det(\mathbf{H}) = 0. \quad (4.3)$$

Similar conditions have been used to study electromechanical instability in dielectric elastomers (Zhao & Suo 2007; Diaz-Calleja *et al.* 2008; Leng *et al.* 2009; Dorfmann & Ogden 2010; Xu *et al.* 2010; Bertoldi & Gei 2011).

The homogeneous deformation as discussed in §3 includes stable and unstable states. By condition (4.3), the unstable state can be readily determined. For example, in figure 3*a*, between the peak and the valley voltages, there are three homogeneous states, with small, intermediate and large axial stretches. It can be shown that the state with the intermediate stretch is unstable against small perturbations, while the other two states are stable against small perturbations. However, condition (4.3) does not distinguish stable and metastable states, as the Hessian matrix is positive-definite in either case. To determine the thermodynamically stable state of equilibrium, one searches for the global minimum of the free-energy function, not restricted to small perturbations only. In the case of discontinuous phase transition, the stable equilibrium state changes abruptly at the transition point, which is typically beyond the reach of small perturbation analysis.

5. Electromechanical phase transition

With a prescribed uniaxial force (P_1) and voltage (Φ), the free energy in (2.10) can be written as a function of the stretches (λ_1, λ_2) in a dimensionless form:

$$\frac{\Pi}{\mu L_1 L_2 L_3} = -\frac{J_{\lim}}{2}\log\left(1 - \frac{\lambda_1^2 + \lambda_2^2 + \lambda_1^{-2}\lambda_2^{-2} - 3}{J_{\lim}}\right) - \left(\frac{P_1}{\mu L_2 L_3}\right)\lambda_1 - \frac{1}{2}\left(\frac{\Phi}{L_3}\sqrt{\frac{\varepsilon}{\mu}}\right)^2 (\lambda_1\lambda_2)^2. \tag{5.1}$$

To illustrate how to determine the states of equilibrium and their stability, the free-energy function is plotted in figure 4, for $P_1/(\mu L_2 L_3) = 1$ and $\Phi/(L_3\sqrt{\mu/\varepsilon}) = 0.337$, which has two local minima and one saddle point. The saddle point corresponds to an unstable state. The two local minima correspond to two states of equilibrium deformation, both stable against small perturbations, one with relatively small stretches and the other with relatively large stretches. For convenience, the former is called the 'thick' state and the latter the 'thin' state. When the free energies of the two states are different, the state with the lower free energy is thermodynamically stable, while the other state is metastable. As the force and voltage change, the stable state of the elastomer may change from one state to the other, a typical behaviour of first-order phase transition. This transition however cannot be predicted by the local stability condition in (4.3).

Under special circumstances, the two deformation states of the elastomer may coexist. Following a recent analysis of phase transition in a temperature-sensitive hydrogel (Cai & Suo 2011), we develop the conditions for coexistence of the two states in the elastomer membrane. Suppose that the deformation of the membrane is no longer homogenous, but is composed of regions in two states, thick and thin. The thick state has smaller stretches in both the axial and lateral directions than

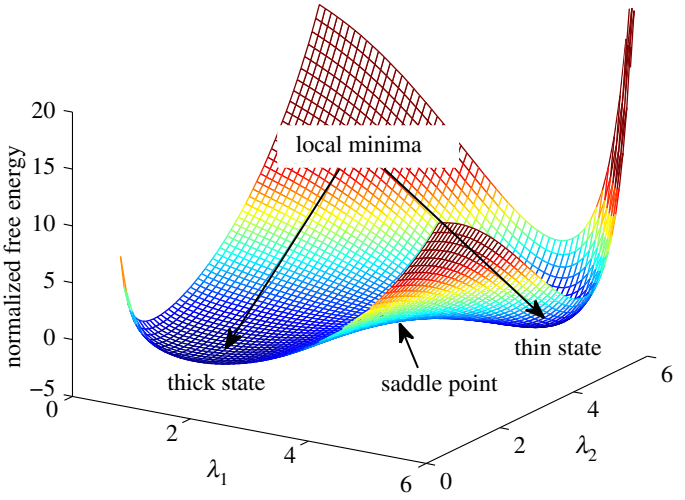

Figure 4. Normalized free energy as a function of the stretches for a dielectric elastomer under a uniaxial force $P_1/(\mu L_2 L_3) = 1$ and a voltage $\Phi/(L_3\sqrt{\mu/\varepsilon}) = 0.337$, showing two local minima and one saddle point. (Online version in colour.)

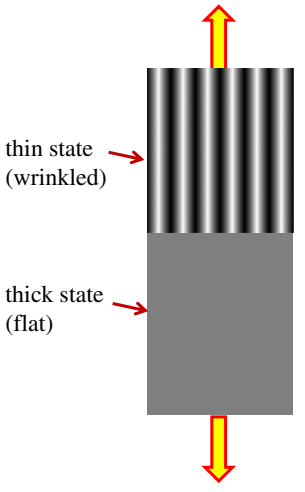

Figure 5. A schematic of two states coexisting in a dielectric elastomer membrane subject to uniaxial tension and voltage. (Online version in colour.)

the thin state. For the two states to coexist, the mismatch in the lateral stretch (λ_2) has to be accommodated geometrically. This may be achieved by wrinkling of the membrane in the thin state, as illustrated in figure 5. With zero force in the lateral direction and negligible bending rigidity of the membrane, wrinkles parallel to the axial direction allow the region in the thin state to have a much larger stretch in the lateral direction than the region in the thick state. The transitional region between the two states, assumed to be much smaller than the

regions in the two states, is neglected in this analysis. In the reference state, the regions of the two states are of lengths L_1' and L_1'', and the total length of the membrane is

$$L_1' + L_1'' = L_1. \tag{5.2}$$

In the current state, the membrane is subject to an axial force P_1 and a voltage Φ. The stretches in the two regions are (λ_1', λ_2') and $(\lambda_1'', \lambda_2'')$, respectively. The total length of the membrane is then

$$L_1'\lambda_1' + L_1''\lambda_1'' = l_1. \tag{5.3}$$

The free energy of the system is

$$\begin{aligned}\Pi = {} & L_2L_3L_1' W_{\mathrm{s}}(\lambda_1', \lambda_2') + L_2L_3L_1'' W_{\mathrm{s}}(\lambda_1'', \lambda_2'') - P_1(L_1'\lambda_1' + L_1''\lambda'') \\ & - \left(\frac{\Phi}{L_3}\right)^2 \frac{\varepsilon}{2} L_2L_3[L_1'(\lambda_1'\lambda_2')^2 + L_1''(\lambda_1''\lambda_2'')^2].\end{aligned} \tag{5.4}$$

When the force and the voltage are held constant, the free energy (5.4) is a function of five independent variables: $\Pi(\lambda_1', \lambda_2', \lambda_1'', \lambda_2'', L_1')$. Associated with variations of the five variables, the free energy varies by

$$\begin{aligned}\delta\Pi = {} & L_2L_3L_1' \left[\frac{\partial W_{\mathrm{s}}(\lambda_1', \lambda_2')}{\partial \lambda_1'} - \frac{P_1}{L_2L_3} - \varepsilon\lambda_1'(\lambda_2')^2\left(\frac{\Phi}{L_3}\right)^2\right]\delta\lambda_1' \\ & + L_2L_3L_1'' \left[\frac{\partial W_{\mathrm{s}}(\lambda_1'', \lambda_2'')}{\partial \lambda_1''} - \frac{P_1}{L_2L_3} - \varepsilon\lambda_1''(\lambda_2'')^2\left(\frac{\Phi}{L_3}\right)^2\right]\delta\lambda_1'' \\ & + L_2L_3L_1' \left[\frac{\partial W_{\mathrm{s}}(\lambda_1', \lambda_2')}{\partial \lambda_2'} - \varepsilon(\lambda_1')^2\lambda_2'\left(\frac{\Phi}{L_3}\right)^2\right]\delta\lambda_2' \\ & + L_2L_3L_1'' \left[\frac{W_{\mathrm{s}}(\lambda_1'', \lambda_2'')}{\partial \lambda_2''} - \varepsilon(\lambda_1'')^2\lambda_2''\left(\frac{\Phi}{L_3}\right)^2\right]\delta\lambda_2'' \\ & + L_2L_3\left[W_{\mathrm{s}}(\lambda_1', \lambda_2') - W_{\mathrm{s}}(\lambda_1'', \lambda_2'') - \frac{P_1}{L_2L_3}(\lambda_1' - \lambda_1'')\right. \\ & \left. - \frac{1}{2\varepsilon}\left(\frac{\Phi}{L_3}\right)^2((\lambda_1'\lambda_2')^2 - (\lambda_1''\lambda_2'')^2)\right]\delta L_1'.\end{aligned} \tag{5.5}$$

For the current state to be a state of stable equilibrium, the free energy in (5.4) shall be minimized. As a necessary condition, the coefficients in front of the five variations in (5.5) must vanish, giving that

$$\frac{P_1}{L_2L_3} + \varepsilon\lambda_1'(\lambda_2')^2\left(\frac{\Phi}{L_3}\right)^2 = \frac{\partial W_{\mathrm{s}}(\lambda_1', \lambda_2')}{\partial \lambda_1'}, \tag{5.6}$$

$$\frac{P_1}{L_2L_3} + \varepsilon\lambda_1''(\lambda_2'')^2\left(\frac{\Phi}{L_3}\right)^2 = \frac{\partial W_{\mathrm{s}}(\lambda_1'', \lambda_2'')}{\partial \lambda_1''}, \tag{5.7}$$

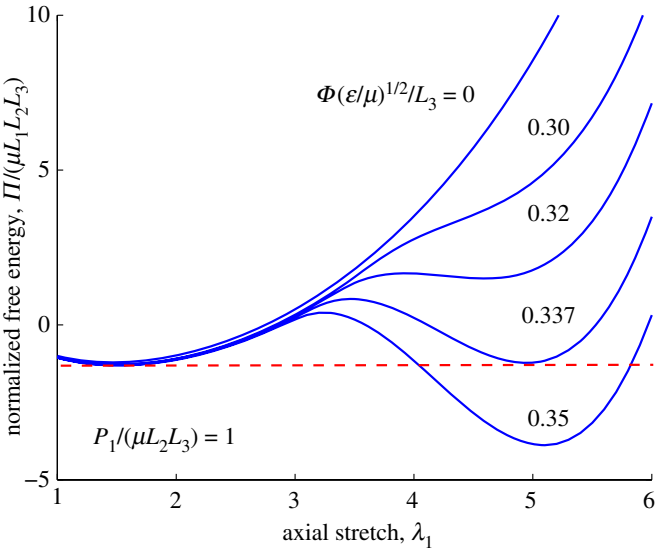

Figure 6. The free energy as a function of the axial stretch for a dielectric elastomer membrane subject to increasing voltage, with a constant uniaxial force. (Online version in colour.)

$$\varepsilon(\lambda_1')^2\lambda_2'\left(\frac{\Phi}{L_3}\right)^2 = \frac{\partial W_s(\lambda_1', \lambda_2')}{\partial \lambda_2'}, \tag{5.8}$$

$$\varepsilon(\lambda_1'')^2\lambda_2''\left(\frac{\Phi}{L_3}\right)^2 = \frac{W_s(\lambda_1'', \lambda_2'')}{\partial \lambda_2''} \tag{5.9}$$

and

$$W_s(\lambda_1', \lambda_2') - \frac{P_1}{L_2 L_3}\lambda_1' - \frac{\varepsilon}{2}\left(\frac{\Phi}{L_3}\right)^2(\lambda_1'\lambda_2')^2 = W_s(\lambda_1'', \lambda_2'') - \frac{P_1}{L_2 L_3}\lambda_1'' - \frac{\varepsilon}{2}\left(\frac{\Phi}{L_3}\right)^2(\lambda_1''\lambda_2'')^2. \tag{5.10}$$

Equations (5.6–5.10) are the conditions for the two states to coexist and equilibrate with each other in the membrane. By (5.6) and (5.7), the axial force in the two states equal to the applied force, which is simply force balance in the axial direction. By (5.8) and (5.9), the lateral forces in both states vanish as required by the boundary condition. Therefore, equations (5.6)–(5.9) simply recover the homogeneous solution in (3.1) and (3.2) for each state. With reference to (2.10), we note that by (5.10), the nominal densities of the free energy in the two states are equal, a condition for the two states to coexist in addition to the requirement that each state be stable against small perturbations.

To illustrate the process of electromechanical phase transition in the dielectric elastomer, we plot in figure 6 the normalized free-energy density (5.1) as a function of the axial stretch λ_1 subject to a constant uniaxial force $P_1/(\mu L_2 L_3) = 1$. As shown in figure 2, the lateral stretch λ_2 is uniquely determined for each axial stretch under a prescribed force. Consequently, λ_2 can be solved as a function of λ_1

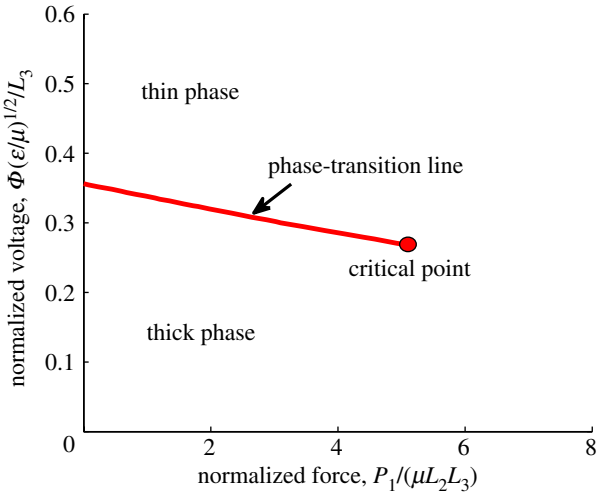

Figure 7. An electromechanical phase diagram for a dielectric elastomer membrane subject to uniaxial force and voltage. The phase-transition line separates regions of two phases—the thick phase and the thin phase, and terminates at the critical point. (Online version in colour.)

by (3.1) for the prescribed uniaxial force, reducing the independent variables in (5.1) to one. When the voltage is low, e.g. $\Phi/(L_3\sqrt{\mu/\varepsilon}) = 0.3$, the free-energy density as a function of λ_1 has a single minimum, corresponding to a stable thick state of homogeneous deformation. As the voltage increases, another local minimum appears at a much larger stretch, corresponding to the thin state. When $\Phi/(L_3\sqrt{\mu/\varepsilon}) = 0.32$, the free-energy density of the thin state is higher than the thick state. Thus, the thick state remains stable and the thin state is metastable. When $\Phi/(L_3\sqrt{\mu/\varepsilon}) = 0.337$, the free-energy densities in the two states are equal; the two states may coexist. Further increasing the voltage results in a transition of the stable state from the thick state to the thin state. Apparently, such a transition resembles a discontinuous first-order phase transition, and the transition voltage can be determined by the condition for coexistence of the two states in (5.6)–(5.10).

The transition voltage as a function of the prescribed force is plotted in figure 7, which represents an electromechanical phase diagram on the force–voltage plane. Below the transition line, the thick state of the elastomer is stable; above the transition line, the thin state is stable. The two states may coexist when the force and voltage are on the transition line, which is determined by (5.6–5.10). Interestingly, the transition line terminates at a critical point, $P_1/(\mu L_2 L_3) = 5.1$ and $\Phi/(L_3\sqrt{\mu/\varepsilon}) = 0.268$ for $J_{\lim} = 69$; no phase transition is predicted beyond the critical point. As shown in figure 3*a*, when the force is small (subcritical), $P_1/(\mu L_2 L_3) < 5.1$, there exists a local maximum and a local minimum in the voltage-stretch curve, and the transition voltage is in between. On the other hand, when $P_1/(\mu L_2 L_3) > 5.1$ (supercritical), the voltage-stretch curve becomes monotonic, and the homogeneous solution is unique and stable for all voltages. Therefore, following a supercritical path in the phase diagram, the membrane can undergo a succession of gradual changes from one state to another, whereas

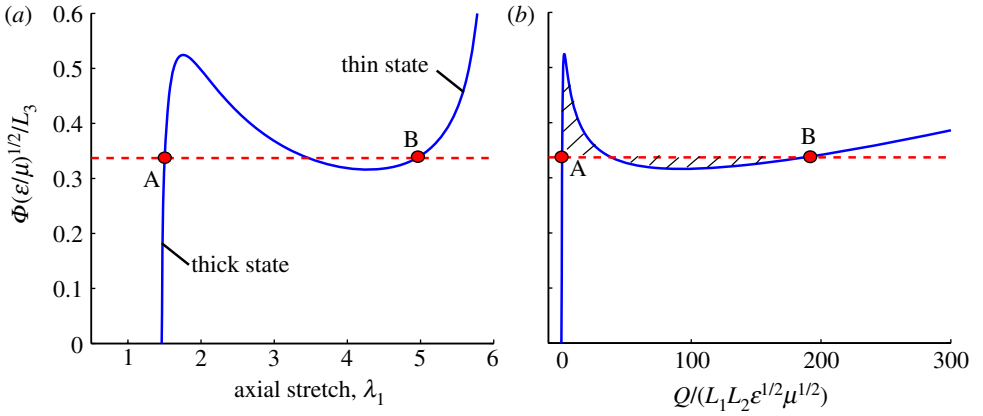

Figure 8. Voltage-induced phase transition under a constant force $P_1/(\mu L_2 L_3) = 1$, with a transition voltage at $\Phi\sqrt{\varepsilon/\mu}/L_3 = 0.337$. (Online version in colour.)

a discontinuous phase transition occurs along a subcritical loading path. The electromechanical phase diagram, with the presence of a critical point, is a close reminiscent of the pressure–temperature diagram for liquid-vapour phase transition of pure substances (Cengel & Boles 2010).

With reference to figure 7, we discuss two types of phase transition in the dielectric elastomer. First, for a membrane subject to a constant force, e.g. $P_1/(\mu L_2 L_3) = 1$, phase transition occurs when the applied voltage crosses the transition line in figure 7. As shown in figure 8*a*, the thick state is stable below the transition voltage, $\Phi/(L_3\sqrt{\mu/\varepsilon}) = 0.337$, and the thin state is stable above the transition voltage. The transition between the two states, from A to B or vice versa, is indicated by the horizontal line. Figure 8*b* shows the normalized charge versus the voltage. The total charge accumulated in the electrodes changes drastically before and after the phase transition. It can be shown that, for the states A and B to have equal free-energy density, the shaded area above the transition voltage in figure 8*b* must be equal to the shaded area below the transition voltage, which is the well-known Maxwell's rule in thermodynamics of a pure substance (Wisniak & Golden 1998).

For the second type of phase transition, consider a membrane subject to a constant voltage, e.g. $\Phi/(L_3\sqrt{\mu/\varepsilon}) = 0.3$. In this case, phase transition occurs when the applied force crosses transition line in figure 7. As shown in figure 9*a*, the thick state is stable below the transition force, $P_1/(\mu L_2 L_3) = 3.1$, while the thin state is stable above the transition force. Figure 9*b* plots the normalized charge versus the force. Again, the transition between the two states, from A to B or vice versa, results in a drastic change in the total charge. By Maxwell's rule, the shaded area above the transition force in figure 9*a* equals the shaded area below the transition force. As can be seen from the phase diagram in figure 7, the force-induced phase transition occurs only when the voltage is within a window, $0.268 < \Phi/(L_3\sqrt{\mu/\varepsilon}) < 0.356$ for $J_{\lim} = 69$.

Figure 10 plots phase diagrams on planes of different coordinates. As a common practice in thermodynamics, various phase-transition processes can be represented graphically using these diagrams. The phase-transition line in figure 7

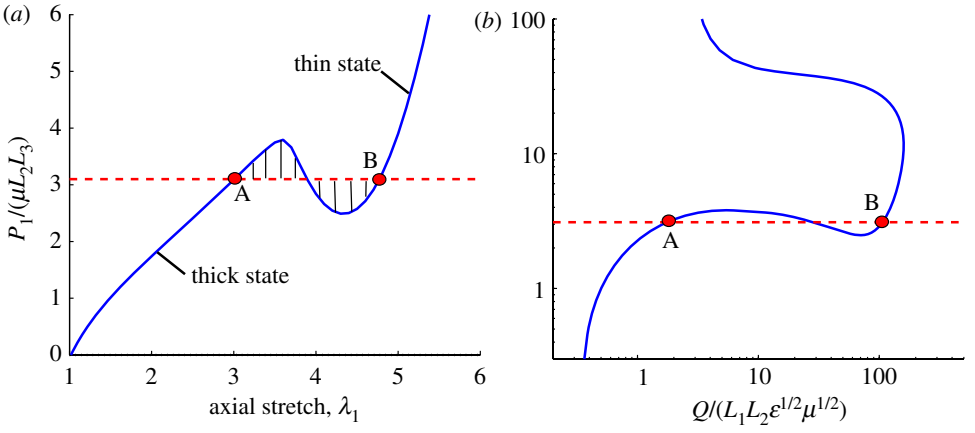

Figure 9. Force-induced phase transition under a constant voltage, $\Phi\sqrt{\varepsilon/\mu}/L_3 = 0.3$, with a transition force at $P_1/(\mu L_2 L_3) = 3.1$. (Online version in colour.)

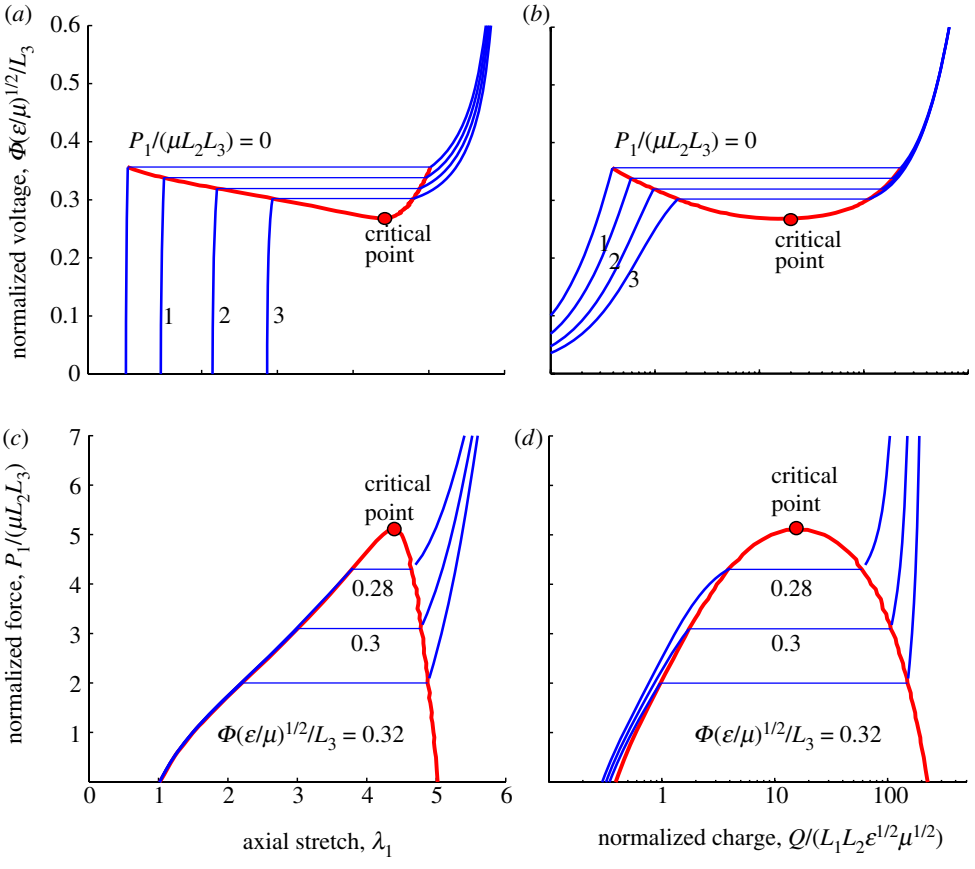

Figure 10. Electromechanical phase diagrams in different coordinates. (a,b) Phase transition under constant axial forces; (c,d) phase transition under constant voltages. (Online version in colour.)

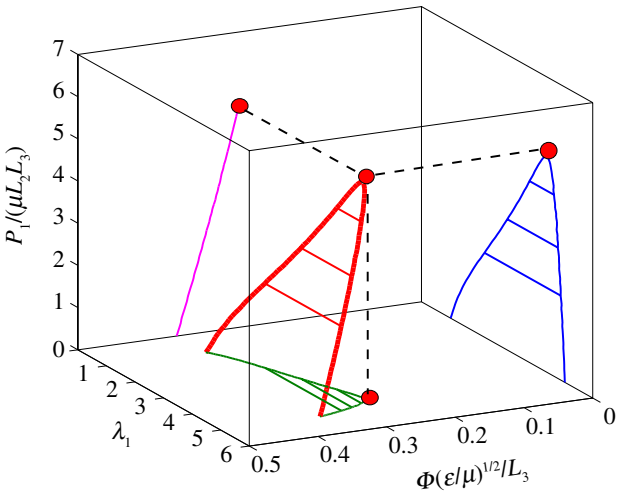

Figure 11. A three-dimensional representation of the electromechanical phase diagram for a dielectric elastomer membrane. (Online version in colour.)

splits into two branches in each of the four diagrams in figure 10. Each diagram consists of two single-phase regions and a region in between for mixture of two states. In particular, the processes of voltage-induced phase transition under the condition of constant forces are represented by the horizontal lines in figure 10*a*,*b*. Similarly, the force-induced phase transition processes under constant voltages are represented by the horizontal lines in figure 10*c*,*d*. For each horizontal line, the two ends represent the two homogeneous states (thick and thin), analogous to the saturated liquid and vapour phases of a pure substance. In between, the two states coexist, with a specific proportion depending on the average stretch or the average charge density. The familiar lever rule can be used to determine the proportion of each phase at any point on the horizontal line, as discussed in §6.

In analogy to the liquid–vapour transition of a pure substance, the deformation state of the dielectric elastomer is determined by two independent variables. For example, with the voltage and the axial stretch as the independent variables, the axial force is determined and the behaviour of the elastomer can be represented as a surface in the three-dimensional space, $P_1 - \lambda_1 - \Phi$, similar to the pressure–volume–temperature (P–v–T) surface in thermodynamics. Figure 11 shows the transition line in the three-dimensional diagram. The two-dimensional diagrams ($P_1 - \Phi$ in figure 7, $\Phi - \lambda_1$ in figure 10*a* and $P_1 - \lambda_1$ in figure 10*c*) are simply the two-dimensional projections of the three-dimensional diagram onto corresponding planes.

6. Discussions

(*a*) *Phase transition with a fixed axial stretch*

As depicted in figure 5, when the thick and thin states coexist in an elastomer membrane, the region in the thin state forms wrinkles to accommodate the mismatch with the thick state in the lateral stretch. Wrinkling of an elastomer

membrane was observed in experiments by Plante & Dubowsky (2006), where the membrane was under a fixed biaxial pre-stretch. Now consider a slightly different condition, where the elastomer membrane is first stretched by a uniaxial force and subsequently subject to increasing voltage with the total axial stretch fixed. No constraint is imposed on the lateral stretch so that the uniaxial stress condition is maintained in the membrane. With reference to the phase diagram in figure 10*a*, as the voltage increases, the deformation state of the elastomer changes along a vertical path in the $\Phi - \lambda_1$ plane. The membrane is in a stable homogeneous state before it reaches the transition line. Slightly above the transition line, the membrane bifurcates into two states, thick and thin, with the region in the thin state wrinkled. As the voltage increases, each state evolves along the transition line, with the axial stretch decreasing in the thick state (λ_1') and increasing in the thin state (λ_1''). To maintain the fixed total stretch (λ_1^{tot}), it requires that

$$L_1'\lambda_1' + L_1''\lambda_1'' = L_1\lambda_1^{\mathrm{tot}}. \tag{6.1}$$

Combining (6.1) with (5.2) gives the volume fractions of the two states:

$$\frac{L_1'}{L_1} = \frac{\lambda_1^{\mathrm{tot}} - \lambda_1''}{\lambda_1' - \lambda_1''} \quad \text{and} \quad \frac{L_1''}{L_1} = \frac{\lambda_1^{\mathrm{tot}} - \lambda_1'}{\lambda_1'' - \lambda'}, \tag{6.2}$$

which is the familiar lever rule. Consequently, the volume fractions of the two states evolve with increasing voltage.

Figure 12*a* plots the evolution of axial stretches with a fixed total stretch $\lambda_1^{\mathrm{tot}} = 2$, and the volume fraction of the thin state is shown in figure 12*b*. In this case, the phase transition starts at $\Phi/(L_3\sqrt{\mu/\varepsilon}) = 0.325$, beyond which the volume fraction of the thin state increases as the voltage increases. Meanwhile, as shown in figure 12*c*, the axial force in the membrane drops abruptly, following the transition line from A to B. At $\Phi/(L_3\sqrt{\mu/\varepsilon}) = 0.356$, the axial force becomes zero, corresponding to a slack state of the membrane. Further increasing the voltage, no homogeneous solution exists for the thick state, and thus the membrane takes on a homogeneous thin state. However, since the axial stretch in the thin state is much larger than the prescribed total stretch, the elastomer membrane buckles, resulting in essentially zero force in the axial direction. As shown in figure 12*b*, the volume fraction of the thin state undergoes a continuous transition at A and a discontinuous transition at B. Figure 12*d* plots the normalized total charge ($Q = D'L_1'L_2 + D''L_1''L_2$) in the electrodes as a function of the applied voltage. Over the entire process in this case, as the end-to-end distance of the membrane is fixed, no mechanical work is done by the elastomer, while the voltage does electrical work to increase the internal free energy of the elastomer (pumping charge onto the electrodes). An inverse process would convert the internal free energy to do electrical work (e.g. charging a battery).

(*b*) *Phase transition with an open circuit*

Analogous to the adiabatic process in thermodynamics, we next consider the electromechanical process in a dielectric elastomer membrane under an open-circuit condition for which the total charge in the electrodes is conserved. The charge may be pumped onto the electrodes by a battery when the elastomer membrane is subject to zero force ($P_1 = 0$). Depending on the voltage of the

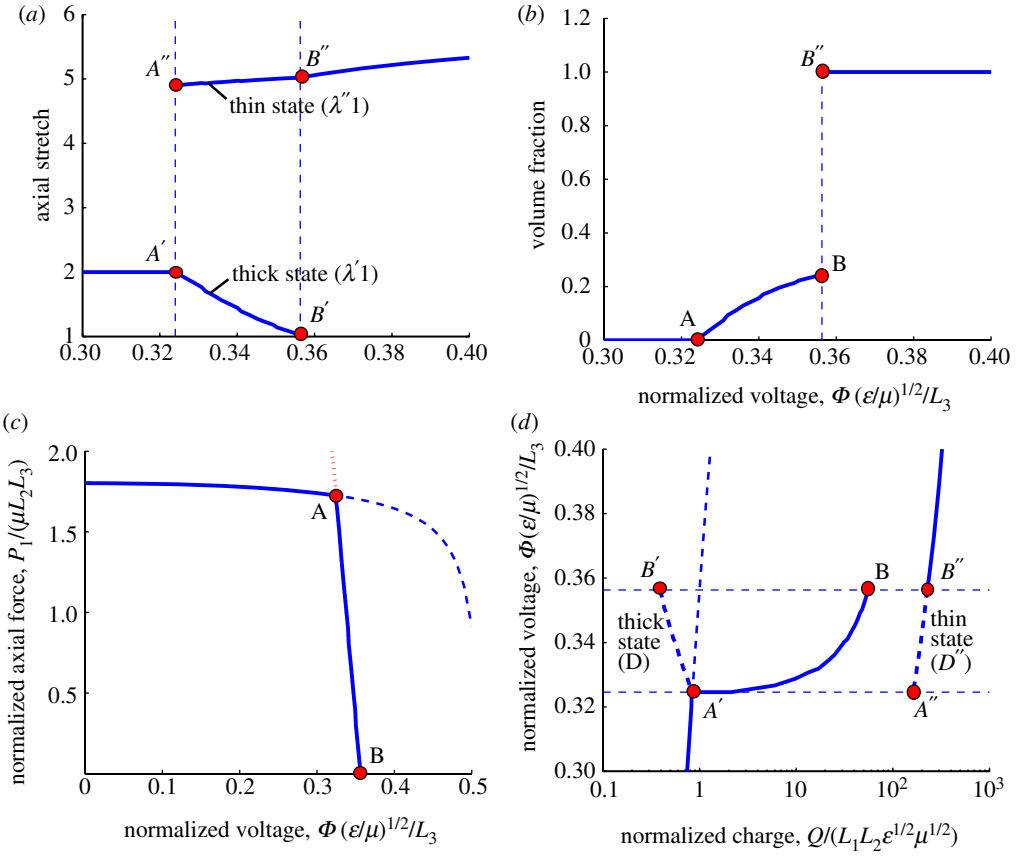

Figure 12. Phase transition of a pre-stretched dielectric elastomer membrane. (*a*) The axial stretch bifurcates into two branches ($A'B'$ and $A''B''$) during phase transition, while the average stretch remains constant ($\lambda_1^{\mathrm{tot}} = 2$). (*b*) The volume fraction of the thin state undergoes a continuous transition at point A and a discontinuous transition at B. (*c*) The axial force decreases as the voltage increases. The dashed line shows the homogeneous solution, which becomes unstable at the transition voltage (point A). (*d*) The normalized charge versus normalized voltage. The nominal charge density bifurcates into two states at the transition voltage and evolves along two separate branches (the thick dashed lines), while the total charge follows the solid line from A to B. (Online version in colour.)

battery, the membrane may be in a single state (thick or thin) or a mixture of two states (figure 10*b*). With a prescribed total charge, the state or the volume fraction of each state in the mixture is uniquely determined. At this point, disconnect the membrane from the battery and load the membrane with a uniaxial force. With reference to figure 10*d*, as the force increases, the voltage decreases, following a vertical path in the $P_1 - Q$ plane. When the prescribed charge is in the range $0.4 < Q/(L_1 L_2 \sqrt{\mu\varepsilon}) < 225$, the membrane is a mixture of two states before the force is applied. With increasing force, the charge density in each state evolves, and the volume fraction can be obtained by a lever rule similar to (6.2),

$$\frac{L_1'}{L_1} = \frac{Q/(L_1 L_2) - D''}{D' - D''} \quad \text{and} \quad \frac{L_1''}{L_1} = \frac{Q/(L_1 L_2) - D'}{D'' - D'}, \tag{6.3}$$

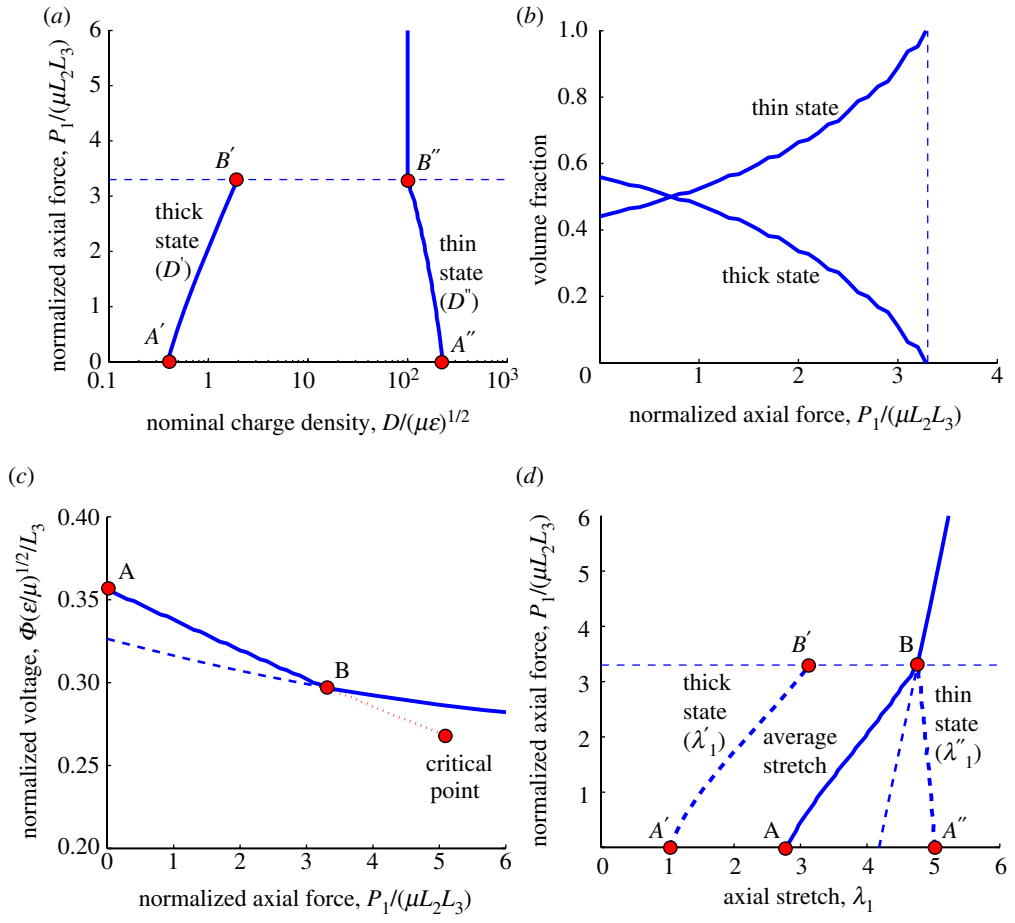

Figure 13. Phase transition under open-circuit condition in a charged dielectric elastomer membrane. (*a*) The nominal charge density has two branches ($A'B'$ and $A''B''$) for the two coexistent states, while the total charge remains a constant, $Q/(L_1 L_2\sqrt{\mu\varepsilon}) = 100$. (*b*) Evolution of the volume fractions of the two states. (*c*) Normalized axial force versus voltage, initially following the transition line from A to B, with a mixture of two states. Beyond B, the elastomer is in a single homogeneous state. The dashed line shows the homogeneous solution, which is unstable below the transition force (point B). (*d*) Axial stretch versus normalized force: the stretches in the two states are shown as the thick dashed lines and the average stretch is shown as the thick solid line. (Online version in colour.)

where $D' = Q'/(L'_1 L_2)$, $D'' = Q''/(L''_1 L_2)$, Q' and Q'' are the charge accumulated on the electrodes over the two homogeneous states. Eventually, the membrane takes on a single-phase homogeneous state when the force is sufficiently high.

As an example, figure 13*a* shows the evolution of charge densities (D' and D'') in the thick and thin states, with a prescribed total charge $Q/(L_1 L_2\sqrt{\mu\varepsilon}) = 100$. The volume fractions are plotted in figure 13*b*. In the voltage–force plane (figure 13*c*), the voltage decreases with increasing force, first following the transition line from A to B and then the homogeneous solution for the thin state. Figure 13*d* plots the total axial stretch versus the axial force. The total stretch

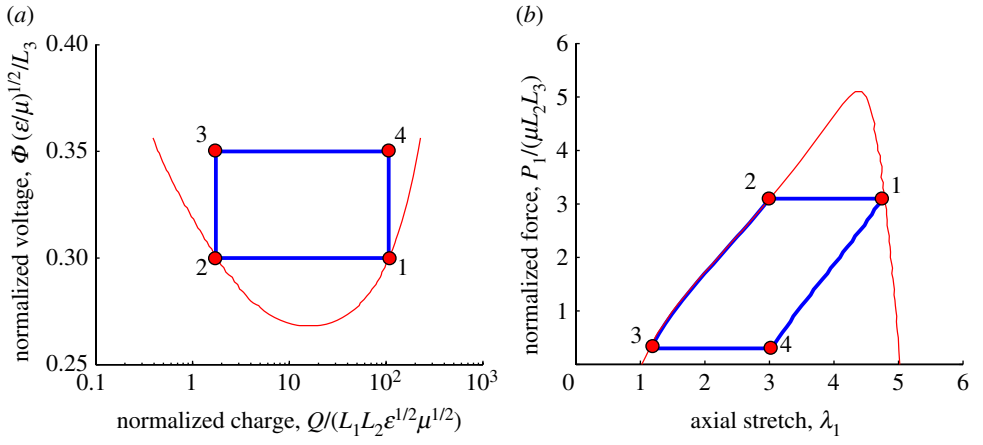

Figure 14. A reversible cycle for electromechanical energy conversion: (*a*) voltage–charge diagram and (*b*) axial force–stretch diagram. Process 1–2: reversible iso-voltage contraction at a low voltage (Φ_{L}) and a high force (P_{H}); process 2–3: reversible iso-charge contraction with an open circuit; process 3–4: reversible iso-voltage charging at a high voltage (Φ_{H}) and a low force (P_{L}); process 4–1: reversible iso-charge stretching with an open circuit. The area within the cycle in the voltage–charge diagram is the net input electric work, and the area in the force–stretch cycle is the net output mechanical work. (Online version in colour.)

is obtained from the axial stretches in the thick and thin states by (6.1), with the volume fraction determined by (6.3). During this process, the axial force does mechanical work to the membrane. Part of this work brings the opposite charges on electrodes closer so that the voltage decreases, analogous to the temperature change in an adiabatic process in classical thermodynamics.

(*c*) *Electromechanical energy conversion*

To discuss electromechanical energy conversion in the elastomer membrane, we construct a cycle of reversible processes analogous to the Carnot cycle in thermodynamics, as shown in figure 14 ($P_1 - \lambda_1$ and $\Phi - D$ diagrams). Similar cycles have been described by Koh *et al.* (2009, 2011) without considering the electromechanical phase transition. Here, we extend the discussion to include the phase transition, which may significantly increase the amount of electromechanical energy conversion. The four reversible processes that make up the cycle are described as follows.

Process 1–2: reversible iso-voltage contraction with a low voltage (Φ_{L}) and a large force (P_{H}). The electrodes of the elastomer membrane are connected to a battery that serves as a reservoir of electric charges and maintains a constant voltage. The membrane is highly stretched at state 1 (e.g. by hanging a large weight) and tends to contract by electromechanical phase transition from 1 to 2. As charges flow from the electrodes to the battery, the average axial stretch of the membrane decreases. During this process, the membrane does both mechanical work by pulling the weight and electric work by charging the battery.

Process 2–3: reversible iso-charge contraction with an open circuit. At state 2, disconnect the electrodes from the battery so that the total charge is conserved.

By gradually reducing the axial force to P_L (state 3), the membrane continues to contract, doing mechanical work. Meanwhile, the voltage increases from Φ_L to Φ_H. This is an inverse process to that discussed in §6*b*.

Process 3–4: reversible iso-voltage charging with a high voltage (Φ_H) and a low force (P_L). At state 3, connect the electrodes to another battery of voltage Φ_H. As the membrane is being stretched by the force P_L, charges flow from the battery to the electrodes until the total charge equals the charge in state 1. During this process, external work is done to the membrane by both mechanical stretching and electric charging.

Process 4–1: reversible iso-charge stretching with an open circuit. At state 4, disconnect the battery again and gradually increase the weight to stretch the membrane further. As the average stretch increases, the voltage drops from Φ_H to Φ_L, returning to state 1 and closing the cycle. This process is similar to that discussed in §6*b*.

The area enclosed by the path of the process cycle (1–2–3–4–1) in the P_1–λ_1 diagram (figure 14*b*) is the net mechanical work done to the weights by the elastomer membrane, while the area enclosed by the path in the Φ–D diagram (figure 14*a*) is the net electric work done to the elastomer membrane by the batteries. As a result, the electrical energy is converted to do mechanical work in this cycle. As all processes in the cycle are reversible, an inverse cycle (4-3-2-1-4) may be used to convert mechanical energy to charge the battery. Like the Carnot cycle, thermodynamically reversible cycles cannot be achieved in practice because the irreversibility associated with the processes cannot be completely eliminated. However, the theoretical heat engine that operates on the Carnot cycle is the most efficient engine operating between two specific temperature limits. Similarly, a reversible cycle as depicted in figure 14 is the most efficient cycle operating between two specific voltage limits for electromechanical energy conversion by the dielectric elastomer membrane.

(*d*) *Electrical breakdown*

One physical limit for the elastomer membrane as an electromechanical transducer is electrical breakdown when the true electrical field reaches a critical value (Kollosche & Kofod 2010). For the electromechanical phase transition to occur without electrical breakdown, the true electrical field in the thin state must be lower than the breakdown field. This is also a necessary condition for the reversible cycle in figure 14 to operate. Otherwise, the net energy that can be converted by the elastomer membrane is drastically reduced as the process cycle is limited within the region of the thick state in the P_1–λ_1 and Φ–D diagrams (figure 10*b*,*c*). In particular, the thick state is stable in a very narrow region in the P_1–λ_1 diagram (figure 1*c*), meaning that very little mechanical work can be done by the elastomer membrane without phase transition, although the deformation can be large.

Consider the breakdown field (E_B) as an intrinsic material property of the dielectric elastomer, which sets an upper limit for the true electrical field, namely, $\Phi/\lambda_3 L_3 < E_B$. In the dimensionless form, we have

$$\frac{\Phi}{L_3}\sqrt{\frac{\varepsilon}{\mu}} < \frac{E_B}{\lambda_1\lambda_2}\sqrt{\frac{\varepsilon}{\mu}}. \tag{6.4}$$

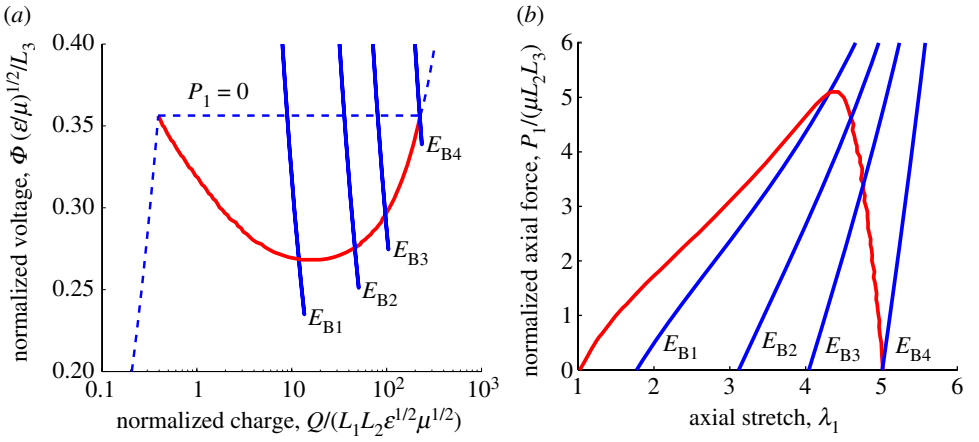

Figure 15. Electrical breakdown limits in (*a*) voltage–charge and (*b*) force–stretch diagrams, for $E_B\sqrt{\varepsilon/\mu} = 1.785$ (E_{B1}), 3.570 (E_{B2}), 5.355 (E_{B3}) and 8.925 (E_{B4}). The red curves are the electromechanical phase-transition lines ($J_{lim} = 69$). (Online version in colour.)

Figure 15 plots the electrical breakdown limits in the voltage–charge and force–stretch diagrams, along with the electromechanical phase-transition lines. Each thick blue line represents the limit by one particular value of the normalized breakdown field. The intersection between the line of electrical breakdown (blue) and the line of phase transition (red) in the voltage–charge diagram sets the upper limit for the voltage in the thin state of the elastomer membrane. The similar intersection in the force–stretch diagram sets the lower limit for the axial force in the thin state. Electromechanical phase transition may occur without electrical breakdown under the condition of high axial force and low voltage. When the normalized breakdown field is sufficiently high (e.g. $E_B\sqrt{\varepsilon/\mu} = 8.925$), the entire transition line is in the region of no breakdown, and thus can be used for electromechanical energy conversion. The normalized breakdown field may be increased by increasing the dielectric permittivity (ε) of the elastomer while maintaining low mechanical stiffness (μ) and high breakdown field (E_B), as demonstrated recently by Stoyanov *et al.* (2010).

7. Summary

We present a theoretical analysis on electromechanical phase transition of dielectric elastomers. A phase diagram is constructed for a dielectric elastomer membrane under uniaxial force and voltage, with two states of deformation (thick and thin), exhibiting a close resemblance to the phase diagram for liquid–vapour phase transition of a pure substance. In particular, a critical point is identified in the electromechanical phase diagram, with which both subcritical and supercritical loading paths can be devised for the membrane to deform from one state to another. The processes of phase transition under various conditions are discussed. A reversible process cycle is suggested for electromechanical energy conversion using the dielectric elastomer membrane, analogous to the Carnot

cycle for a heat engine. However, using the electromechanical phase transition for energy conversion may be limited by failure of the dielectric elastomer owing to electrical breakdown. With a particular combination of the material properties (e.g. $E_{\mathrm{B}}\sqrt{\varepsilon/\mu}$ and J_{lim}), electromechanical phase transition can be used to significantly enhance the amount of energy conversion by dielectric elastomer transducers.

R.H. gratefully acknowledges partial support of this work by the University of Texas at Austin through the Faculty Research Assignment programme and the travel support to visit Harvard University by Moncrief Grand Challenge Award from the Institute of Computational Engineering and Science at the University of Texas. Z.S. is supported by the NSF through a grant on Soft Active Materials (CMMI-0800161), and by the MURI through a contract on Adaptive Structural Materials (W911NF-09-1-0476).

References

Bertoldi, K. & Gei, M. 2011 Instabilities in multilayered soft dielectrics. *J. Mech. Phys. Solids* **59**, 18–42. (doi:10.1016/j.jmps.2010.10.001)

Boyce, M. C. & Arruda, E. M. 2000 Constitutive models of rubber elasticity: a review. *Rubber Chem. Technol.* **73**, 504–523. (doi:10.5254/1.3547602)

Brochu, P. & Pei, Q. B. 2010 Advances in dielectric elastomers for actuators and artificial muscles. *Macromol. Rapid Commun.* **31**, 10–36. (doi:10.1002/marc.200900425)

Cai, S. & Suo, Z. 2011 Mechanics and chemical thermodynamics of a temperature-sensitive hydrogel. *J. Mech. Phys. Solids* **59**, 2259–2278. (doi:10.1016/j.jmps.2011.08.008)

Calvert, P. 2009 Hydrogels for soft machines. *Adv. Mater.* **21**, 743–756. (doi:10.1002/adma.200800534)

Carpi, F., Rossi, D. D., Kornbluh, R., Pelrine, R. & Sommer-Larsen, P. 2008 *Dielectric elastomers as electromechanical transducers: fundamentals, materials, devices, models and applications of an emerging electroactive polymer technology.* Amsterdam, The Netherlands: Elsevier.

Carpi, F., Bauer, S. & Rossi, D. D. 2010 Stretching dielectric elastomer performance. *Science* **330**, 1759–1761. (doi:10.1126/science.1194773)

Cengel, Y. A. & Boles, M. A. 2010 *Thermodynamics*, 7th edn. New York: McGraw Hill.

Diaz-Calleja, R., Riande, E. & Sanchis, M. J. 2008 On electromechanical stability of dielectric elastomers. *Appl. Phys. Lett.* **93**, 101902. (doi:10.1063/1.2972124)

Dorfmann, A. & Ogden, R. W. 2005 Nonlinear electroelasticity. *Acta Mech.* **174**, 167–183. (doi:10.1007/s00707-004-0202-2)

Dorfmann, A. & Ogden, R. W. 2010 Nonlinear electroelastics: incremental equations and stability. *Int. J. Eng. Sci.* **48**, 1–14. (doi:10.1016/j.ijengsci.2008.06.005)

Gent, A. N. 1996 A new constitutive relation for rubber. *Rubber Chem. Technol.* **69**, 59–61. (doi:10.5254/1.3538357)

Goulbourne, N. C. Mockensturm, E. M. Frecker, M. 2005 A nonlinear model for dielectric elastomer membranes. *ASME J. Appl. Mech.* **72**, 899–906. (doi:10.1115/1.2047597)

Ha, S. M. Yuan, W., Pei, Q. B. Pelrine, R. & Stanford, S. 2007 Interpenetrating networks of elastomers exhibiting 300% electrically induced area strain. *Smart Mater. Struct.* **16**, S280–287. (doi:10.1088/0964-1726/16/2/S12)

Kofod, G., Sommer-Larsen, P., Kornbluh, R. & Pelrine, R. 2003 Actuation response of polyacrylate dielectric elastomers. *J. Intell. Mater. Syst. Struct.* **14**, 787–793. (doi:10.1177/104538903039260)

Koh, S. J. A., Zhao, X. & Suo, Z. 2009 Maximal energy that can be converted by a dielectric elastomer generator. *Appl. Phys. Lett.* **94**, 262902. (doi:10.1063/1.3167773)

Koh, S. J. A., Keplinger, C., Li, T. F., Bauer, S. & Suo, Z. 2011 Dielectric elastomer generators: how much energy can be converted? *IEEE/ASME Trans. Mechatron.* **16**, 33–41. (doi:10.1109/TMECH.2010.2089635)

Kollosche, M. & Kofod, G. 2010 Electrical failure of chemically identical, soft thermoplastic elastomers with different elastic stiffness. *Appl. Phys. Lett.* **96**, 071904. (doi:10.1063/1.3319513)

Leng, J. S., Liu, L. W., Liu, Y. J., Yu, K. & Sun, S. H. 2009 Electromechanical stability of dielectric elastomers. *Appl. Phys. Lett.* **94**, 211901. (doi:10.1063/1.3138153)

Li, B., Chen, H., Qiang, J., Hu, S., Zhu, Z. & Wang, Y. 2011 Effect of mechanical pre-stretch on the stabilization of dielectric elastomer actuation. *J. Phys. D: Appl. Phys.* **44**, 155301. (doi:10.1088/0022-3727/44/15/155301)

Liu, F. & Urban, M. W. 2010 Recent advances and challenges in designing stimuli-responsive polymers. *Progr. Polym. Sci.* **35**, 3–23. (doi:10.1016/j.progpolymsci.2009.10.002)

McMeeking, R. M. & Landis, C. M. 2005 Electrostatic forces and stored energy for deformable dielectric materials. *J. Appl. Mech.* **72**, 581–590. (doi:10.1115/1.1940661)

Pelrine, R., Kornbluh, R., Pei, Q. B. & Joseph, J. 2000 High-speed electrically actuated elastomers with strain greater than 100%. *Science* **287**, 836–839. (doi:10.1126/science.287.5454.836)

Plante, J. S. & Dubowsky, S. 2006 Large-scale failure modes of dielectric elastomer actuators. *Int. J. Solids Struct.* **43**, 7727–7751. (doi:10.1016/j.ijsolstr.2006.03.026)

Shankar, R., Ghosh, T. K. & Spontak, R. J. 2007 Dielectric elastomers as next-generation polymeric actuators. *Soft Matter* **3**, 1116–1129. (doi:10.1039/b705737g)

Stark, K. H. & Garton, C. G. 1955 Electric strength of irradiated polythene. *Nature* **176**, 1225–1226. (doi:10.1038/1761225a0)

Stoyanov, H., Kollosche, M., McCarthy, D. N. & Kofod, G. 2010 Molecular composites with enhanced energy density for electroactive polymers. *J. Mater. Chem.* **20**, 7558–7564. (doi:10.1039/c0jm00519c)

Suo, Z. 2010 Theory of dielectric elastomers. *Acta Mech. Sol. Sin.* **23**, 549–578. (doi:10.1016/S0894-9166(11)60004-9)

Suo, Z., Zhao, X. & Greene, W. H. 2008 A nonlinear field theory of deformable dielectrics. *J. Mech. Phys. Solids* **56**, 467–286. (doi:10.1016/j.jmps.2007.05.021)

Tommasi, D. D., Puglisi, G., Saccomandi, G. & Zurlo, G. 2010 Pull-in and wrinkling instabilities of electroactive dielectric actuators. *J. Phys. D: Appl. Phys.* **43**, 325501. (doi:10.1088/0022-3727/43/32/325501)

Trimarco, C. 2009 On the Lagrangian electrostatics of elastic solids. *Acta Mech.* **204**, 193–201. (doi:10.1007/s00707-008-0056-0)

Wisniak, J. & Golden, M. 1998 Predicting saturation curve of a pure substance using Maxwell's rule. *J. Chem. Educ.* **75**, 200–203. (doi:10.1021/ed075p200)

Wissler, M. & Mazza, E. 2005 Modeling and simulation of dielectric elastomer actuators. *Smart Mater. Struct.* **14**, 1396–1402. (doi:10.1088/0964-1726/14/6/032)

Xu, B.-X., Mueller, R., Classen, M. & Gross, D. 2010 On electromechanical stability analysis of dielectric elastomer actuators. *Appl. Phys. Lett.* **97**, 162908. (doi:10.1063/1.3504702)

Zhao, X. & Suo, Z. 2007 Method to analyze electromechanical stability of dielectric elastomers. *Appl. Phys. Lett.* 91, 061921. (doi:10.1063/1.2768641)

Zhao, X., Hong, W. & Suo, Z. 2007 Electromechanical coexistent states and hysteresis in dielectric elastomers. *Phys. Rev.* B **76**, 134113. (doi:10.1103/PhysRevB.76.134113)

Zhou, J. X., Hong, W., Zhao, X. & Suo, Z. 2008 Propagation of instability in dielectric elastomers. *Int. J. Solids Struct.* **45**, 3739–3750. (doi:10.1016/j.ijsolstr.2007.09.031)